

# A novel heterodimeric cysteine protease is required for interleukin-1 $\beta$ processing in monocytes

Nancy A. Thornberry\*, Herbert G. Bull\*, Jimmy R. Calaycay†, Kevin T. Chapman‡, Andrew D. Howard†, Matthew J. Kostura§, Douglas K. Miller†, Susan M. Molineaux||, Jeffrey R. Weidner†, John Aunins¶, Keith O. Elliston#, Julia M. Ayala†, Francesca J. Casano||, Jayne Chin§, Gloria J.-F. Ding†, Linda A. Egger†, Erin P. Gaffney\*, Guadalupe Limjoco§, Oksana C. Palyha†, S. M. Raju†, Anna M. Rolando||, J. Paul Salley†, Ting-Ting Yamin†, Terry D. Lee\*\*, John E. Shively\*\*, Malcolm MacCross‡, Richard A. Mumford†, John A. Schmidt† & Michael J. Tocci||††

Departments of \* Biochemistry, † Biochemical and Molecular Pathology, ‡ Medicinal Chemical Research, § Cellular and Molecular Pharmacology, || Molecular Immunology, ¶ Biochemical Process Research and Development, and # Biological Data, Merck Research Laboratories, PO Box 2000, Rahway, New Jersey 07065, USA

\*\* Beckman Research Institute City of Hope, 1450 East Duarte Road, Duarte, California 91010, USA

Interleukin-1 $\beta$  (IL-1 $\beta$ )-converting enzyme cleaves the IL-1 $\beta$  precursor to mature IL-1 $\beta$ , an important mediator of inflammation. The identification of the enzyme as a unique cysteine protease and the design of potent peptide aldehyde inhibitors are described. Purification and cloning of the complementary DNA indicates that IL-1 $\beta$ -converting enzyme is composed of two nonidentical subunits that are derived from a single proenzyme, possibly by autoproteolysis. Selective inhibition of the enzyme in human blood monocytes blocks production of mature IL-1 $\beta$ , indicating that it is a potential therapeutic target.

INTERLEUKIN-1 (IL-1) is a major mediator in the pathogenesis of chronic and acute inflammatory disease. Evidence that IL-1 is an excellent target for therapeutic intervention has been obtained using macromolecules acting as receptor antagonists (IL-1RA (refs 1–4), soluble IL-1R (ref. 5), anti-IL-1R monoclonal antibodies<sup>6</sup>). But, attempts to identify low-molecular-weight receptor antagonists suitable for oral therapy have been uniformly unsuccessful. Thus another approach, amenable to the design and synthesis of small molecules, is needed.

IL-1 $\beta$ , the predominant form of IL-1 released by human monocytes, is synthesized as an inactive 33K or 31K ( $M_r$  33,000 or 31,000) precursor (pIL-1 $\beta$ )<sup>7,8</sup>. The fully active 17.5K mature form of IL-1 $\beta$  (mIL-1 $\beta$ ) begins at Ala 117 and therefore seems to result from processing between Asp 116 and Ala 117 (refs 9, 10). This unique site for prohormone processing is located in an evolutionarily conserved sequence in all known IL-1 $\beta$  molecules<sup>11</sup>. An IL-1 $\beta$ -converting enzyme (ICE) activity has been identified in monocytes and THP.1 cells which cleaves pIL-1 $\beta$  at Asp 116–Ala 117 as well as Asp 27–Gly 28 to yield products of 17.5K and 28K, respectively<sup>12,13</sup>. Cleavage at each site is dependent on aspartic acid in the P<sub>1</sub> position<sup>12,14,15</sup>. Moreover, ICE seems to be a pIL-1 $\beta$ -specific processing enzyme because it does not cleave IL-1 $\alpha$  or several other proteins containing many Asp–X bonds<sup>14</sup>. This unique specificity should allow the development of selective inhibitors of ICE.

Here we describe the purification, cloning, specificity, and investigations into the catalytic mechanism of ICE. Potent and selective inhibitors have also been used to affinity-purify active

enzyme to homogeneity from THP.1 cell lysates, and to prove the role of ICE in the processing of pIL-1 $\beta$ .

## Purification

ICE was purified from the cytosol of the human monocytic cell line THP.1 by a three-step high-performance liquid chromatography (HPLC) procedure. Sequential fractionation of the cytosolic material over DEAE-5PW and SP-5PW yielded congruent single peaks of ICE activity as measured by cleavage of radiolabelled human pIL-1 $\beta$ <sup>12</sup>, a 14-amino-acid peptide spanning the pIL-1 $\beta$  cleavage site<sup>14</sup>, or the fluorogenic substrate described below. SDS-polyacrylamide gel electrophoresis (SDS-PAGE) of the SP-5PW peak fractions indicated that two polypeptides with  $M_r$  of 22K and 10K consistently chromatographed with ICE activity (Fig. 1a). Several preparations purified on SP-5PW also contained small amounts of a protein that migrated with an  $M_r$  of 24K (p24) on SDS-PAGE (results not shown). Each fraction containing ICE activity was individually fractionated by reversed-phase HPLC. Two peaks, neither of which retained enzymatic activity (not shown), were observed in direct proportion to the amount of ICE activity injected onto the column. Analysis of the peaks by SDS-PAGE showed that the first peak contained the 22K protein, and the second the 10K protein, in homogeneous form (Fig. 1b). Roughly 700 pmol of each protein were purified from  $1 \times 10^{11}$  cells.

Relative molecular masses for the 22K and 10K proteins were determined by on-line liquid chromatography/mass spectral analysis using electrospray ionization<sup>15</sup>. The average  $M_r$  values of the purified proteins were 19,866 (Fig. 1c) and 10,248 (Fig. 1d), respectively, and these were designated p20 and p10.

## Substrate specificity

Peptides that span the cleavage site of pIL-1 $\beta$  are suitable substrates for ICE and have been used to define its substrate specificity<sup>14,16</sup>. Two features of peptide substrates are essential for catalytic recognition by the enzyme. First, there is a strong preference for aspartic acid adjacent to the cleavage site, in that any substitution of this residue in pIL-1 $\beta$  and peptide substrates leads to a substantial reduction in the rate of catalysis ( $>100$ -fold)<sup>14,16</sup>. The results in Fig. 2 indicate that there is an equally stringent requirement ( $>100$ -fold) for four amino-acid residues to the left of the cleavage site, whereas methylamine is sufficient to the right. The results also indicate that broad substitution is tolerated in the P<sub>2</sub> position (peptides 18–24); this has been exploited in the design of peptide substrates and inhibitors described below. The minimal substrate for the enzyme, Ac-Tyr-Val-Ala-Asp-NH-CH<sub>3</sub> (peptide 16; AC, acetyl), is the best peptide substrate yet identified for the enzyme, having a relative

†† To whom correspondence should be addressed.

$V_{\max}/K_m$  comparable to that for pIL-1 $\beta$  ( $12 \pm 2$  versus  $10 \pm 4$  for pIL-1 $\beta$ ).

These features are embodied in the fluorogenic substrate, Ac-Tyr-Val-Ala-Asp-7-AMC (peptide 17; AMC, amino-4-methylcoumarin). Cleavage of this substrate shows Michaelis-Menten kinetics with  $K_m = 14 \pm 3 \mu\text{M}$ . The continuous, fluorometric assay developed with this substrate has facilitated a detailed investigation of the catalytic mechanism of the enzyme.

### Classification as a cysteine protease

ICE is inactivated by thiol alkylating reagents<sup>13</sup>. The enzyme is also inhibited by 1,10-phenanthroline (our unpublished observations); however, the mechanism of inhibition is not due to chelation of an active-site metal, but rather to contamination of the phenanthroline with Cu(II) and concomitant metal-catalysed oxidation of an essential thiol<sup>17</sup>. Although such data indicate that the enzyme contains accessible structural and/or catalytic thiol(s), this does not permit assignment of ICE to a protease class.

Three lines of evidence now clearly identify ICE as a cysteine protease. First, and most compelling, is that a diazomethylketone designed with the appropriate active site specificity (Ac-Tyr-Val-Ala-Asp-COCHN<sub>2</sub>, inhibitor A) is a potent, competitive, irreversible inhibitor of the enzyme. Diazomethylketones are highly selective, covalent inhibitors of cysteine proteases<sup>18</sup>. Addition of ICE to reaction mixtures containing  $1 \times K_m$  substrate and 250 nM inhibitor A resulted in time-dependent inhibition of the enzyme (Fig. 3a). Irreversible inhibition was demonstrated by the lack of recovery of activity when saturating levels of substrate ( $10 \times K_m$ ) were added to the completely inhibited reaction. The inhibition is strictly competitive, as indicated by the protection against inactivation observed in the presence of saturating substrate ( $70 \times K_m$ ). The second order rate constant for inactivation,  $1.64 \pm 0.03 \times 10^4 \text{ M}^{-1} \text{ s}^{-1}$ , is comparable to those of the best diazomethylketone inhibitors of other cysteine proteases<sup>18,19</sup>. A 10,000-fold smaller value was obtained for the truncated inhibitor Cbz-Asp-COCHN<sub>2</sub> (Cbz represents carbobenzyloxy group), consistent with substrate specificity studies.

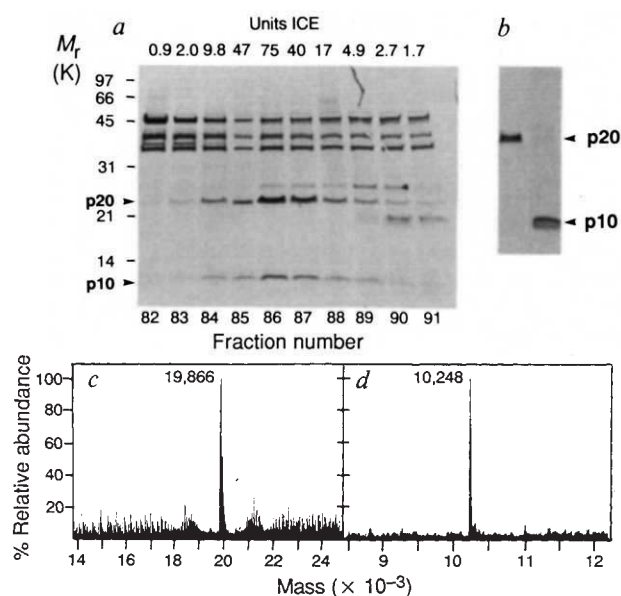


FIG. 1 Identification of ICE proteins. *a*, SDS-PAGE (17–27%) and silver staining of SP-5PW ICE peak fractions (82–91). ICE activity in each fraction as measured in the fluorogenic assay is shown over each lane. Arrows indicate the positions of the 22K and 10K bands that correlated with ICE activity. *b*, SDS-PAGE and silver staining of p20 and p10 ICE proteins purified by reversed-phase HPLC (RP-HPLC). *c*, *d*, The mass of each subunit was determined by mass spectrometry<sup>15</sup>; *c*, 22K subunit (p20); and *d*, 10K subunit (p10).

**METHODS.** *a*, *b*, ICE activity was measured as described previously<sup>14</sup> and in Fig. 2 legend. THP.1 cells were grown in batch fermenters in Iscove's medium supplemented with 9% horse serum and 0.1–0.3% F68 pluronic, washed in PBS, and broken by dounce homogenization in hypotonic buffer containing 25 mM HEPES, pH 7.5, 5 mM MgCl<sub>2</sub>, and 1 mM EGTA, 1 mM PMSF and  $10 \mu\text{g ml}^{-1}$  pepstatin and leupeptin. After differential centrifugation, the cytosolic extract was clarified by filtration through a 0.22- $\mu\text{m}$  filter, dialysed overnight (5 °C) with 20 mM Tris, pH 7.8, 10% sucrose, 0.1% CHAPS, and 2 mM DTT (TSCD buffer). Total protein (3–5 g), corresponding to 1,000 ml cytosolic extract, was applied to a 475-ml bed volume DEAE-5PW HPLC column and eluted with TSCD buffer and a gradient of 0.4 M NaCl and 240 mM Tris-HCl (pH 7.8). Fractions from the DEAE column (50–150 mg) were pooled, diluted with an equal volume of HSCD buffer (contains 25 mM HEPES instead of Tris), adjusted to pH 7.0, applied to a 150-ml bed volume SP-5PW HPLC column and eluted with KCl. Aliquots of SP-5PW fractions were injected onto a narrow bore C4 RP-HPLC column and eluted with a linear gradient of 0.06% trifluoroacetic acid in acetonitrile/H<sub>2</sub>O. *c*, *d*, RP-HPLC-purified p20 and p10 (5 pmol) were analysed by capillary liquid chromatography coupled to a Finnigan MAT TSQ-700 triple sector quadrupole mass spectrometer equipped with an electrospray ion source<sup>15</sup>.

### Amino-terminal truncations

Peptide	P7	P6	P5	P4	P3	P2	P1	P1'	P2'	P3'	P4'	P5'	P6'	P7'	Relative $V_{\max}/K_m$
1	Asn	Glu	Ala	Tyr	Val	His	Asp	Ala	Pro	Val	Arg	Ser	Leu	Asn	1.00 $\pm$ 0.05
2		Glu	Ala	Tyr	Val	His	Asp	Ala	Pro	Val	Arg	Ser	Leu	Asn	0.64 $\pm$ 0.01
3			Ala	Tyr	Val	His	Asp	Ala	Pro	Val	Arg	Ser	Leu	Asn	0.29 $\pm$ 0.02
4				Tyr	Val	His	Asp	Ala	Pro	Val	Arg	Ser	Leu	Asn	0.12 $\pm$ 0.00
5				Ac-Tyr	Val	His	Asp	Ala	Pro	Val	Arg	Ser	Leu	Asn	0.81 $\pm$ 0.01
6					Ac-Val	His	Asp	Ala	Pro	Val	Arg	Ser	Leu	Asn	<0.005
7						His	Asp	Ala	Pro	Val	Arg	Ser	Leu	Asn	<0.005
8							Asp	Ala	Pro	Val	Arg	Ser	Leu	Asn	<0.005

### Carboxy-terminal truncations

Peptide	P7	P6	P5	P4	P3	P2	P1	P1'	P2'	P3'	P4'	P5'	P6'	P7'	Relative $V_{\max}/K_m$
1	Asn	Glu	Ala	Tyr	Val	His	Asp	Ala	Pro	Val	Arg	Ser	Leu	Asn	1.00 $\pm$ 0.05
9	Asn	Glu	Ala	Tyr	Val	His	Asp	Ala	Pro	Val	Arg	Ser	Leu		1.22 $\pm$ 0.16
10	Asn	Glu	Ala	Tyr	Val	His	Asp	Ala	Pro	Val	Arg	Ser			0.80 $\pm$ 0.16
11	Asn	Glu	Ala	Tyr	Val	His	Asp	Ala	Pro	Val	Arg				0.88 $\pm$ 0.04
12	Asn	Glu	Ala	Tyr	Val	His	Asp	Ala	Pro	Val					1.02 $\pm$ 0.09
13	Asn	Glu	Ala	Tyr	Val	His	Asp	Ala	Pro						1.25 $\pm$ 0.15
14	Asn	Glu	Ala	Tyr	Val	His	Asp	Ala							<0.05
15	Asn	Glu	Ala	Tyr	Val	His	Asp	Ala-CO-NH <sub>2</sub>							0.93 $\pm$ 0.03
16				Ac-Tyr	Val	Ala	Asp-NH-CH <sub>3</sub>								12.00 $\pm$ 2.00
17				Ac-Tyr	Val	Ala	Asp-AMC								1.9 $\pm$ 0.1

### P2 substitutions

Peptide	P7	P6	P5	P4	P3	P2	P1	P1'	P2'	P3'	P4'	P5'	P6'	P7'	Relative $V_{\max}/K_m$
18				Ac-Tyr	Val	Ala	Asp	Gly	Trp-NH <sub>2</sub>						6.6 $\pm$ 0.1
19				Ac-Tyr	Val	His	Asp	Gly	Trp-NH <sub>2</sub>						5.4 $\pm$ 1
20				Ac-Tyr	Val	Gln	Asp	Gly	Trp-NH <sub>2</sub>						4.0 $\pm$ 0.3
21				Ac-Tyr	Val	Lys	Asp	Gly	Trp-NH <sub>2</sub>						2.5 $\pm$ 0.3
22				Ac-Tyr	Val	Phe	Asp	Gly	Trp-NH <sub>2</sub>						1.6 $\pm$ 0.1
23				Ac-Tyr	Val	Gln	Asp	Gly	Trp-NH <sub>2</sub>						0.59 $\pm$ 0.08
24				Ac-Tyr	Val	Asp	Asp	Gly	Trp-NH <sub>2</sub>						0.34 $\pm$ 0.03

FIG. 2 Substrate specificity studies. Peptides that span the cleavage site of pIL-1 $\beta$  were evaluated as substrates and used to define the enzyme's minimum recognition sequence. Values for  $V_{\max}/K_m$  are expressed relative to peptide 1 and represent the mean  $\pm$  s.d. ( $n=2-4$ ). The results indicate that peptide 16 is the minimum recognition sequence for ICE, and that broad substitution is tolerated in P<sub>2</sub>.

**METHODS.** Peptides 1–16 and 18–24 were synthesized using the Merrifield solid-phase technique, purified by RP-HPLC, and confirmed by mass spectral analysis. The fluorogenic substrate, Ac-Tyr-Val-Ala-Asp-AMC (peptide 17), was prepared by conventional solution-phase peptide synthesis. The enzyme used in these studies was purified 100-fold using DEAE ion-exchange chromatography as described in Fig. 1. Peptide cleavage reactions contained 50 units enzyme (1 unit = 1 pmol AMC per min at saturating concentrations of peptide 17) and were done as previously described<sup>14</sup>. In the case of pIL-1 $\beta$ , substrate (33K) and product (17.5K) were separated by SDS-PAGE<sup>12</sup>, and quantitated using a radioanalytical imaging system (Ambis Systems).



Second, inactivation of the enzyme by iodoacetate is competitive with substrate (not shown). Competitive inactivation was also demonstrated with other reagents, including cystamine (2-aminoethanethiol disulphide) and glutathione disulphide. Finally, consistent with the enhanced reactivity of catalytic cysteines found in other cysteine proteases<sup>18</sup>, the catalytically essential cysteine reacts with [<sup>14</sup>C]iodoacetate more than 10 times faster than do other cysteines or dithiothreitol (not shown).

The selective and competitive inactivation by [<sup>14</sup>C]iodoacetate was used to identify the active-site cysteine. On the basis of the rate constant for inactivation of free enzyme by iodoac-

tate ( $20 \text{ M}^{-1} \text{ s}^{-1}$ ), conditions were chosen for 99% inactivation in the absence of substrate and only 2% in the presence of saturating levels ( $200 \times K_m$ ). The labelling patterns shown in Fig. 3b were obtained with enzyme purified 10,000-fold by DEAE-cellulose and sulphydrylpropyl chromatography. Coomassie blue staining of the gel indicated about 10 major proteins, of which only two, p20 and a band of higher  $M_r$ , underwent significant <sup>14</sup>C-carboxymethylation. Of these, only p20 was protected by saturating substrate. This established that the catalytically essential cysteine is located in the p20 subunit. Sequencing of a tryptic digest indicated only a single labelled peptide with the sequence Val-Ile-Ile-Ile-Gln-Ala-Cys, with the peak of label coinciding with the cysteine.

### Reversible inhibition by a peptide aldehyde

The catalytic mechanism of the enzyme suggested that peptide aldehydes would be attractive transition-state analogue inhibitors<sup>20</sup>. This was confirmed with the design and synthesis of Ac-Tyr-Val-Ala-Asp-CHO (inhibitor B), which is a potent, competitive, reversible inhibitor of ICE. It is slow binding, as shown by the slow approach to equilibrium when enzyme was added to reaction mixtures containing inhibitor (50 nM) and  $1 \times K_m$  substrate (Fig. 4a). Competitive and reversible inhibition was indicated by the recovery of activity observed when saturating levels of substrate ( $10 \times K_m$ ) were added to fully inhibited enzyme. The behaviour of this inhibitor is consistent with a kinetic model in which the rates of association ( $k_{on}$ ) and dissociation ( $k_{off}$ ) of enzyme-inhibitor complex are slow compared to rate constants for interaction with the substrate<sup>21</sup>. The  $k_{on}$  ( $3.8 \pm 0.3 \times 10^5 \text{ M}^{-1} \text{ s}^{-1}$ ) and  $k_{off}$  ( $2.9 \pm 0.4 \times 10^{-4} \text{ s}^{-1}$ ) define the overall dissociation constant for the equilibrium:  $K_i = k_{off}/k_{on} = 0.76 \pm 0.16 \text{ nM}$ . A  $P_3$ -substituted aldehyde used as a control in whole-blood studies (see below), Ac-Tyr-D-Ala-Ala-Asp-CHO (inhibitor C), has a 1,000-fold reduced affinity for the enzyme ( $K_i = 1.5 \pm 0.1 \mu\text{M}$ ).

### Affinity purification

Affinity chromatography was used to purify active enzyme to homogeneity and to demonstrate the selectivity of the peptide aldehyde inhibitors. The inhibitor Ac-Tyr-Val-Lys-Asp-CHO (inhibitor D), containing lysine at  $P_2$ , was synthesized as an affinity ligand and shown to have somewhat lower affinity ( $K_i = 3 \text{ nM}$ ) than the original aldehyde, as predicted from substrate studies (Fig. 2, peptide 21).

As anticipated from the enzyme's unusual specificity, the immobilized peptide aldehyde proved to be very selective. Affinity chromatography of a crude THP.1 lysate isolated only two proteins, with  $M_r$  values corresponding to p20 and p10 (Fig. 4b). Analysis of affinity-purified enzyme by reversed-phase HPLC and amino-terminal sequence analysis indicated that the subunits are present in equimolar ratio (assuming equal extinction coefficients at 214 nm), and confirmed their identity with those described in Fig. 1. Cleavage of internally labelled pIL-1 $\beta$ <sup>12</sup> by affinity-purified ICE yielded mIL-1 $\beta$  with Ala 117 at the N terminus. The affinity chromatography represents a purification of >100,000-fold in a single step. Besides demonstrating the singular specificity of the peptide aldehyde inhibitors, this affinity method provided the first preparations of pure, catalytically active enzyme.

### Kinetic evidence that ICE is an oligomer

ICE displays kinetic properties of a dissociable multimeric protein in that the enzyme inactivates on dilution. Dilution of the enzyme by 1,000-fold into a sample containing  $1 \times K_m$  substrate results in time-dependent loss of activity ( $t_{1/2} = 2.7 \pm 0.4 \text{ h}$ ; Fig. 4c). Reconstitution (1,000-fold) of the dilute, inactive preparation results in complete recovery of activity (Fig. 4c, inset). The most reasonable explanation for this concentration-dependent behaviour is that catalytically active enzyme is composed of at least two subunits and that both subunits are required for

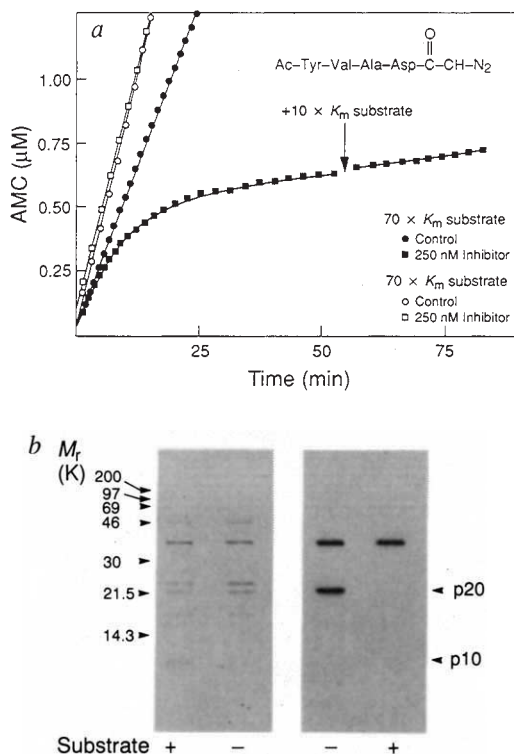


FIG. 3 Evidence that ICE is a cysteine protease. *a*, Inhibition of ICE by the tetrapeptide diazomethylketone, inhibitor A. Addition of peptide A (250 nM) to a reaction mixture containing  $1 \times K_m$  substrate resulted in first-order loss of enzyme activity. The solid line is a theoretical fit to the integrated first-order rate equation developed by Morrison<sup>21</sup>, yielding a value for the first-order rate constant of  $2 \times 10^{-3} \text{ s}^{-1}$ , corresponding to a second-order rate constant of  $1.6 \times 10^4 \text{ M}^{-1} \text{ s}^{-1}$ . The residual activity observed (<3%) represents background cleavage of the substrate due to contaminating proteases. Addition of saturating levels of substrate ( $10 \times K_m$ ) has no influence on the inhibited velocity, indicating irreversible inhibition. To demonstrate competitive inactivation, an identical experiment was done in the presence of saturating substrate ( $70 \times K_m$ ). *b*, Labelling patterns with [<sup>14</sup>C]iodoacetate. ICE was labelled with [<sup>14</sup>C]iodoacetate in the absence (-) and presence (+) of saturating substrate, and analysed by SDS-PAGE. The left-hand lanes are stained with Coomassie blue; the right-hand lanes are autoradiographed. The missing <sup>14</sup>C-labelled band in the substrate-protected case identifies the p20 subunit as containing the active-site cysteine.

**METHODS.** *a*, Ac-Tyr-Val-Ala-Asp-COCHN<sub>2</sub>, inhibitor A, was prepared as follows: aspartic acid diazomethylketone  $\beta$ -methyl ester was coupled to Asp-Tyr-Val-Ala using dicyclohexylcarbodiimide (DCC) and hydroxybenzotriazole (HOBt), and the product hydrolysed with triethylamine and water to yield the final product. Reactions (500  $\mu\text{l}$ ) contained Ac-Tyr-Val-Ala-Asp-AMC (14  $\mu\text{M}$  or 1 mM) and enzyme (25 units) under standard assay conditions. Reactions were monitored continuously in a spectrofluorometer at an excitation wavelength of 380 nm and an emission wavelength of 460 nm. *b*, Labelling was done on sulphydrylpropyl-purified enzyme, in solutions containing 1,400 units  $\text{ml}^{-1}$  enzyme, 100  $\mu\text{M}$  [<sup>14</sup>C]iodoacetate (56 Ci  $\text{mol}^{-1}$ ), in the standard assay buffer<sup>14</sup> (including dithiothreitol) at 25 °C plus or minus 2.8 mM substrate ( $200 \times K_m$ ), for seven half-lives (40 min).

catalytic activity. Dissociation was not observed in the presence of saturating levels of substrate or inhibitor (not shown).

### cDNA cloning

N-terminal and internal tryptic peptide sequences from purified p20 or p10 were used to design degenerate oligonucleotide primers for polymerase chain reaction (PCR) amplification of ICE-specific DNA fragments from THP.1 cell cDNA<sup>22</sup>. Separate PCR products for p20 and p10 were subcloned and used as probes to isolate full-length cDNAs from THP.1 and human monocyte libraries. All of the primary phage isolates hybridized with both probes, demonstrating that both ICE proteins were encoded by the same messenger RNA.

Several cDNAs were sequenced to determine the primary structure of ICE (Fig. 5a, b). There were no significant differences in the cDNA sequences of THP.1 and human monocyte ICE. The longest cDNA insert, which is 1,490 base pairs (bp) long, corresponded to a constitutively expressed, low-abundance transcript (<1:50,000) of 1.6 kilobases (kb) based on northern blot analyses of THP.1 RNA (not shown). The ICE cDNA also hybridized to poly(A) mRNAs of 2.3 and 0.5 kb. All three ICE mRNAs were detected in several non-monocytic cell types including neutrophils and T-lymphocytes, and the Raji B lymphoblastoid cell line (not shown). Five additional nucleotides compared to that of the longest insert were detected by cDNA primer extension (not shown), suggesting that ICE mRNA has a very short 5' untranslated region (UTR) or secondary structure which limits 5' extension. The most favourable Kozak consensus sequence (GCCATGG)<sup>23</sup> is at nucleotide 8 and is followed by a long open reading frame (ORF) of 1,212 nucleotides, that terminates with the ochre codon, TAA, at nt 1,220. The cDNA encodes a predicted proenzyme of 404 amino acids ( $M_r$  45,158).

A protein with an  $M_r$  of 45K (p45) results from *in vitro* transcription and translation of the full-length ICE cDNA (Fig. 6b, lane 1). Two types of ICE cDNAs were identified which differed in the sequence and length of the 3'UTR, suggesting that ICE transcripts are alternatively spliced (not shown).

### Primary structure

Amino-acid sequence and mass spectrometry information were used to delineate the regions in p45 corresponding to p20 and p10. Sequence analysis also indicated that p24 was an alternately processed form of p20 (Fig. 5a, b). From Edman sequencing, the N termini of p24 and p20 are located at Ser 104 and Asn 120, respectively. The N-terminal region of p45 encodes a 119-residue propeptide, containing three cysteines, which lacks the characteristics of a hydrophobic signal sequence. Its function is not known but it is clear from the affinity purification results that it is not required for enzymatic activity (Fig. 4b). Asp 297 was predicted as the C-terminus of p20 based on the  $M_r$  of the subunit (Fig. 1c), identification by fast-atom bombardment mass spectrometry of an appropriately sized Asp-N peptide (Asp 288–Asp 297), and sequence analysis of this peptide by MS/MS<sup>24</sup>. The conclusion that this peptide lies at the terminus of p20 is consistent with the inability of Asp-N to cleave C-terminal aspartic acid residues. The catalytic cysteine identified by active-site labelling, Cys 285, lies within 13 residues of the C terminus of p20.

Sequence analysis of the purified protein and cDNA demonstrated that p10 begins at Ala 317 and terminates with the end of the ORF at His 404. These assignments indicate that a 19-residue spacer separates the C terminus of p20 from the N terminus of p10. Neither this fragment nor the propeptide has been found in purified ICE preparations.

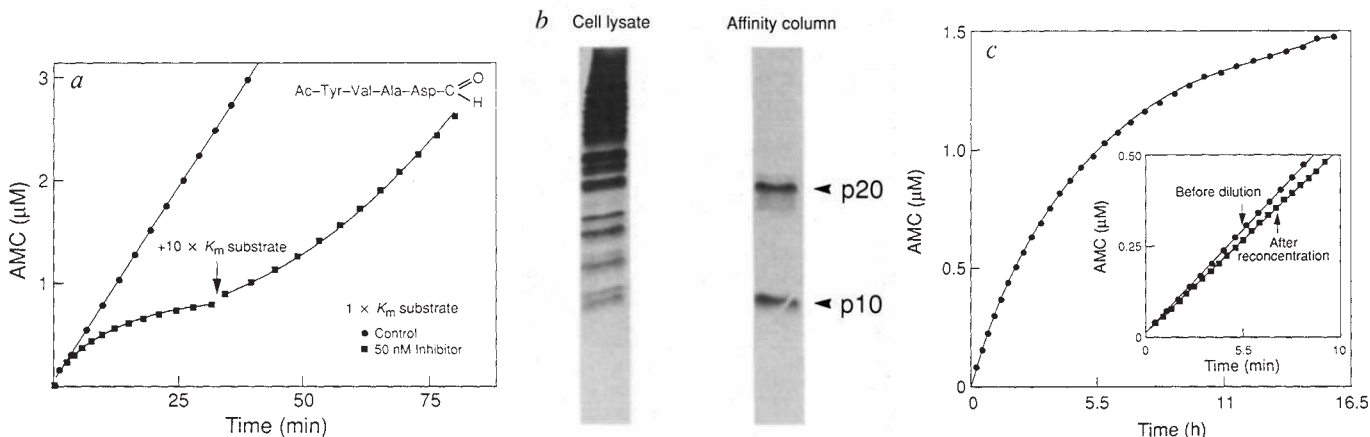
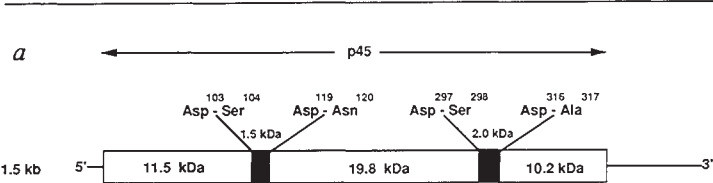


FIG. 4 Potency and selectivity of tetrapeptide aldehydes and evidence that ICE is an oligomer. *a*, Addition of the tetrapeptide aldehyde, peptide B, (50 nM) to a reaction mixture containing  $1 \times K_m$  substrate resulted in time-dependent loss of enzyme activity. Addition of saturating levels of substrate ( $10 \times K_m$ ) to the inhibited reaction resulted in slow, first-order recovery of activity, indicating reversible and competitive inhibition. *b*, Affinity chromatography. Silver-stained SDS-PAGE of THP.1 cell lysate applied to the affinity column, and pure ICE eluted by free inhibitor. The procedure gave ~50% recovery of enzymatic activity, and a purification of >100,000-fold. *c*, Reversible inactivation of ICE by dilution. Enzyme (50  $\mu$ l, 5 units  $\mu$ l<sup>-1</sup>) diluted 1,000-fold into reaction mixtures containing 14  $\mu$ M Ac-Tyr-Val-Ala-Asp-AMC ( $1 \times K_m$ ) undergoes reversible dissociation. The solid line is theoretical for a first-order loss of activity with a rate constant of 0.004 min<sup>-1</sup> (half life, 2.9 h). Less than 2% of the total substrate was consumed over the reaction period. An identical experiment in the absence of sucrose and CHAPS results in a 4-fold faster inactivation rate and both of these components act independently to stabilize the enzyme (not shown). Complete recovery of activity is achieved on 1,000-fold re-concentration of the enzyme. The inset compares the initial velocities before dilution ( $V_0 = 0.057 \mu$ M AMC min<sup>-1</sup>) and after concentration ( $V_0 = 0.051 \mu$ M AMC min<sup>-1</sup>).

METHODS. *a*, Ac-Tyr-Val-Ala-Asp-CHO, peptide B, was prepared as follows:

Alloc-L-aspartic acid  $\beta$ -*t*-butyl ester (Alloc is allyloxycarbonyl) was reduced to the corresponding alcohol through a mixed anhydride using sodium borohydride. The alcohol was oxidized to the aldehyde and converted without purification to the *O*-benzylacetal using trifluoroacetic acid and benzyl alcohol. The Alloc group was removed and the resulting amine coupled *in situ* to Ac-Tyr-Val-Ala using ethyldimethylaminopropylcarbodiimide hydroxybenzotriazole. Hydrogenolysis provided the desired peptide aldehyde. Reactions (500  $\mu$ l) contained Ac-Tyr-Val-Ala-Asp-AMC (14  $\mu$ M or 1,000  $\mu$ M) and enzyme (25 units) under standard assay conditions. The  $k_{on}$ ,  $k_{off}$  and  $K_i$ , were calculated according to ref. 21. *b*, The affinity matrix was prepared by coupling the inhibitor D, protected as its dimethyl acetal, to crosslinked Sepharose 4B by established methods<sup>32</sup>. A lysate from THP.1 cells<sup>12</sup> was equilibrated with an equal volume of affinity gel for 5 h at 4 °C, the gel was washed in a column with 100 volumes standard assay buffer, and the enzyme recovered by exchange with 200  $\mu$ M free inhibitor for 24 h followed by elution with two column volumes of buffer. The enzyme was reactivated by treatment with hydroxylamine and glutathione disulphide, followed by reduction with DTT. *c*, After 20 h, the diluted enzyme (50 ml) was re-concentrated to 50  $\mu$ l using an Amicon ultrafiltration apparatus (YM10 membrane) and a Centricon-10.



### PURIFIED FORMS OF ICE

1 AAAAGGCC ATG GCC GAC AAG GTC CTG AAG GAG AAG AGA AAG CTG TTT ATC CGT TCC ATG GGT GAA GGT  
1▶ Met Ala Asp Lys Val Leu Lys Glu Lys Arg Lys Leu Phe Ile Arg Ser Met Gly Glu Gly

68 ACA ATA AAT GGC TTA CTG GAT GAA TTA TTA CAG ACA AGG GTG CTG AAC AAG GAA GAG ATG GAG AAA  
21▶ Thr Ile Asn Gly Leu Leu Asp Glu Leu Leu Gln Thr Arg Val Leu Asn Lys Glu Glu Met Glu Lys

134 GTA AAA CGT GAA AAT GCT ACA GTT ATG GAT AAG ACC CGA GCT TTG ATT GAC TCT GTT ATT CCG GAA  
43▶ Val Lys Arg Glu Asn Ala Thr Val Met Asp Lys Thr Arg Ala Leu Ile Asp Ser Val Ile Pro Lys

200 GGG GCA GAC GCA TGC CAA ATT TGC ATC ACA TAC ATT TGT GAA GAA GAC AGT TAC CTG GCA GGG AGC  
65▶ Gly Ala Gln Ala Cys Gln Ile Cys Ile Thr Tyr Ile Cys Glu Glu Asp Ser Tyr Leu Ala Gly Thr

226 CTG GGA CTC TCA GCA GAT CAA ACA TCT GGA AAT TAC CTT AAT ATG CAA GAC TCT CAA GGA GTA CTT  
87▶ Leu Gly Leu Ser Ala Asp Gln Thr Ser Gly Asn Tyr Leu Asn Met Gln Asp Ser Gln Gly Val Leu

332 TCT TCC TTT CCA GCT CCT CAG GCA GTG CAG GAC AAC CCA GCT ATT GCC ACA TCC TCA GGC TCA GAA  
109▶ Ser Ser Phe Pro Ala Pro Gln Ala Val Gln Asp Asn Pro Ala Met Pro Thr Ser Ser Gly Ser Glu

398 GGG AAT GTC AAG CTT TGC TCC CTA GAA GAA GCT CAA AGG ATA TGG AAA CAA AAG TCG GCA GAG ATT  
131▶ Gly Asn Val Lys Leu Cys Ser Ser Leu Glu Glu Ala Gln Arg Ile Trp Lys Gln Lys Ser Ala Glu Ile

464 TAT CCA ATA ATG GAC AAG TCA AGC CGC ACA CGT CTT GCT CTC ATT ATC TGC AAT GAA GAA TTT GAC  
153▶ Tyr Pro Ile Met Asp Lys Ser Ser Arg Thr Arg Leu Ala Leu Ile Ile Cys Asn Glu Glu Gly Ile Arg

530 AGT ATT CCT AGA AGA ACT GGA GCT GAG GTT GAC ATC ACA GGC ATG ACA ATG CTG CTA CAA AAT CTG  
175▶ Ser Ile Pro Arg Arg Thr Gly Ala Glu Val Asp Ile Thr Gly Met Thr Met Leu Glu Lys Asn Leu

596 GGG TAC AGC GTA GAT GTG AAA AAA AAT CTC ACT GCT TCG GAC ATG ACT ACA GAG CTG GAG GCA TTT  
197▶ Gly Tyr Ser Val Asp Val Lys Lys Asn Leu Thr Ala Ser Asp Met Thr Thr Glu Glu Ala Phe

662 GCA CAC CGC CCA GAG CAC AAG ACC TCT GAC AGC ACG TCT CTG GTG TTC ATG TCT CAT GGT ATT CGG  
219▶ Ala His Arg Cys Pro Gly His Lys Thr Ser Asp Thr Phe Leu Val Phe Met Ser His Gly Ile Arg

728 GAA GGC ATT TGT GGG AAG AAA CAC TCT GAG CAA GTC CCA GAT ATA CTA CAA CTC AAT GCA ATC TTT  
241▶ Glu Gly Ile Cys Gly Lys Lys His Ser Glu Gln Val Pro Asp Ile Leu Gln Leu Asn Ala Ile Phe

794 AAC ATG TTG AAT ACC AAG AAC TGC CCA AGT TTG AAG GAC AAA CCG AAG GTG ATC ATC ATC CAG GCC  
263▶ Asn Met Leu Asn Thr Lys Asn Cys Pro Ser Leu Lys Asp Lys Pro Lys Val Ile Ile Ile Gln Ala

860 TGC CGT GGT GAC AGC CCT GGT GTG GTG TGG TTT AAA GAT TCA GTA GGA GTT TCT GGA AAC CTA TCT  
285▶ Cys Arg Gly Asp Ser Pro Gly Val Val Trp Phe Lys Asp Ser Val Gly Val Ser Gly Asn Leu Ser

926 TTA CCA ACT ACA GAA GAG TTT GAG GAT GAT GCT ATT AAG AAA GCC CAC ATA GAG AAG GAT TTT ATC  
307▶ Leu Pro Thr Thr Glu Glu Phe Glu Asp Asp Ala Ile Lys Lys Ala His Ile Glu Lys Asp Phe Ile

992 GCT TTC TGC TCT TCC ACA CCA GAT AAT GTT TCT TGG AGA CAT CCC ACA ATG GGC TCT GTT TTT ATT  
329▶ Ala Phe Cys Ser Ser Thr Pro Asp Asn Val Ser Trp Arg His Pro Thr Met Gly Ser Val Phe Ile

1058 GGA AGA CTC ATT GAA CAT ATG CAA GAA TAT GCC TGT TCC TGT GAT GTG GAG GAA ATT TTC CGC AAG  
351▶ Gly Arg Leu Ile Glu His Met Gln Glu Tyr Ala Cys Ser Cys Asp Val Glu Glu Ile Phe Arg Lys

1124 GTT CGA TTT TCA TTT GAG CAG CCA GAT GGT AGA GCG GAG ATG CCC ACC ACT ACA GAA GTG ACT TTG  
373▶ Val Arg Phe Ser Phe Glu Gln Pro Asp Gly Arg Ala Gln Met Pro Thr Thr Glu Arg Val Thr Leu

1190 ACA AGA TGT TTC TAC CTC TTC CCA GGA CAT TAAATTAAGGAACCTGTATGAATGCTCTGGCGAGGGTGAAGAGATC  
395▶ Thr Arg Cys Phe Tyr Leu Phe Pro Gly His OC

1267 CTCCTGTAAGGTTTTTGAAATTGTCTGCTGTAATAAATCTTTTTGAAATATAAATCTGGTAGAAAAATGAIAAAAAAAAAA

1354 AAAAA

C

Cys consensus	-----GX <b>C</b> XG-----
Rhinovirus	---YATKTG <b>C</b> GGVLCATGK---
Poliovirus	---FPTRAG <b>C</b> GGVITCTGKSS
Enterovirus	---FPTKAG <b>C</b> GGVVISMGKIV
Coxsackievirus	---FPTKAG <b>C</b> GGVLMSTGKVL
ICE	VII IQACRGDS <b>E</b> GVVWFKD---
	*
Tissue kallikrein	DGGKDTCVGD <b>S</b> GGPLICDGVLQ
<i>Drosophila</i> protease	DG-KATCGD <b>S</b> GGPLVTKEGDK
Prostate protease	DG-KSTCSGD <b>S</b> GGPLVLCNGVLL
Pancreatic elastase	SG-ASSCGD <b>S</b> GGPLVCEKGD-
Arginine esterase	EGKKTCTCKD <b>S</b> GGPLICDGL-
Ser consensus	-----CXGX <b>S</b> XG-----

FIG. 5. Organization of the human ICE cDNA. *a*, The predicted ORF encoding the ICE proenzyme (p45) is represented by a rectangle. 5' and 3' UTR sequences are shown as solid bars. The four ICE-like cleavage sites flanking the known forms of ICE (p24, p20 and p10) are indicated. The C terminus of p24 has not been determined and is represented by a dashed arrow. *b*, Nucleotide and deduced amino-acid sequence of ICE. Nucleotides are numbered 5' to 3'. The ochre termination codon is designated OC. Primers used for amplification are denoted by bold arrows. Oligonucleotide probes used to characterize the PCR products are indicated by dashed lines. Deduced sequences confirmed by Edman sequencing are underlined (only a subset are shown for clarity). Asp-N-derived peptides are denoted by D. The N termini of p24, p20 and p10 and the C termini of p20 and p10 are indicated by double asterisks. The active-site Cys is boxed. *c*, Alignments of ICE with cellular serine and viral cysteine proteases. ICE is aligned with the highest scoring sequences from the final Profile searches. Serine and viral cysteine active-site consensus sequences<sup>25,26</sup> and the corresponding sequence in ICE are boxed. Shaded boxes indicate the active-site cysteine or serine residues. The asterisk denotes the catalytic Cys 285 of ICE. Serine protease sequences are tissue kallikrein from mouse (A05308), a serine protease from *Drosophila melanogaster* (PSO049), a prostate-specific protease (S03604), pancreatic elastase (A23473), and arginine esterase (S00613). Viral cysteine protease sequences are coxsackie virus (GNNYA9), bovine enterovirus (GNNYBE), poliovirus type 1 (GNNY1P) and human rhinovirus type 14 (GNNYH4).

**METHODS.** *a* and *b*, p20 and p10 were reduced, alkylated and sequenced as described previously<sup>33</sup>. For p20, the N-terminal primer, GAYCCNGCNATGCCNAC, was 128 times degenerate and the internal primer, TTRTCATDATNGRTA, 48 times degenerate (Stanford code<sup>38</sup>). For p10, the N-terminal primer, GCNATHAARAAGCNCA, was 192 times and the internal primer, GTYTACGGNTGNTGNT, 128 times degenerate. Single-stranded THP 1 cDNA was synthesized from poly(A)<sup>+</sup> mRNA and used as a PCR template as described<sup>22</sup>. For p20, a PCR product of 116 bp was confirmed as ICE-specific by hybridization with the oligonucleotide ATIGGRTAATYTCIGCR. A 221-bp PCR product was verified for p10, with the probe ATIGARAARGAYTTYATIGC. Probes were 5' end-labelled and hybridized at 33 °C (15 to 20 °C below *T<sub>m</sub>*) as described previously<sup>34</sup>. The subcloned PCR products were sequenced by the chain termination method<sup>35</sup> and used as hybridization probes in separate screenings of commercial (Clontech) THP.1 (λgt10) or human monocyte (λgt11) cDNA libraries<sup>35</sup>. Positive inserts were subcloned and sequenced on both strands<sup>35</sup>. *c*. Homology searches were conducted with the ICE nucleotide and protein sequences against Genbank<sup>36</sup> and PIR<sup>37</sup> using the GCG package<sup>38</sup>. A non-redundant database<sup>39</sup> was used to generate distinct profiles<sup>40</sup> representing the catalytic regions of cellular serine and viral cysteine proteases. These profiles, designed using alignments suggested in ref. 26, were used to search for similar regions in the primary sequence of ICE. PIR sequence identifiers are bracketed.



The theoretical mass for p20 (Asn 120–Asp 297), assuming all five cysteines including the active-site Cys 285 are reduced, is 19,844. The theoretical mass for p10 (Ala 317–His 404), assuming that all four cysteines are reduced, is 10,244. The mass values determined for p20 (19,866) and p10 (10,248) by on-line liquid chromatography/mass spectral analysis (Fig. 1c, d) are within 0.11 and 0.04%, respectively, of the theoretical values and are in keeping with the accuracy of this technique for proteins of this size (0.01–0.20%)<sup>15</sup>. These results indicate that neither ICE subunit undergoes significant post-translational modification (for example, farnesylation). But the acidic conditions used for reversed-phase HPLC might remove acid-labile groups (such as phosphate). We hypothesize that in non-stimulated THP.1 cells ICE, like pIL-1 $\beta$ <sup>11</sup>, is in the cytosol.

The sequence of ICE is not homologous to any known protein, including cellular cysteine proteases. But Ser 289 of ICE and adjacent residues readily aligns with the consensus sequence (Gly-X-Ser/Cys-X-Gly)<sup>25,26</sup> corresponding to the catalytic regions of serine and viral cysteine proteases (Fig. 5c). Using this alignment, the catalytic cysteine of ICE, Cys 285, aligns with a conserved cysteine which is normally disulphide-linked in serine proteases.

### Functional expression

To verify further the identity of the ICE cDNA, the 1.5-kb insert was cloned into an expression vector, transfected into COS-7 cells, and assayed for ICE activity. Lysates from ICE-transfected cells, but not those from cells transfected with the expression vector alone, cleaved >80% of the pIL-1 $\beta$  to 17.5 and 28K products (Fig. 6a, lanes 1 and 2). The 17.5K cleavage product comigrated with mIL-1 $\beta$  produced by incubation of the substrate with affinity-purified ICE (Fig. 6a, lanes 4 and 5) and was completely inhibited by inhibitor B (Fig. 6a, lane 3). The substrate specificity of the expressed ICE activity was verified by incubating lysates with a pIL-1 $\beta$  cleavage site mutant (Asp 116→Ala) which cannot be cleaved at Ala 116–Ala 117 by ICE<sup>12</sup>. As with native ICE, the activity from the transfectants cleaves the mutant substrate to a 28K product but not to mIL-1 $\beta$  (Fig. 6a, lanes 6 and 7)<sup>12</sup>.

### Processing of p45

The primary sequence of ICE revealed that the N termini of p24 and p10 as well as the N and C termini of p20 result from cleavage of Asp-X bonds, where X equals Ser 104, Asn 120, Ser 298 or Ala 317 (Fig. 5a). Human ICE requires Asp in P<sub>1</sub> and prefers small hydrophobic residues (Gly>Ala>Val) in P<sub>1'</sub> (ref. 14). But not all proteins with Asp-X bonds are cleaved

by ICE, human and murine pIL-1 $\beta$  remaining the only known substrates<sup>14</sup>. Therefore, it was of interest to determine whether active ICE could cleave the proenzyme. The primary ICE translation product, p45, is stable in rabbit reticulocyte lysates for at least 24 h (Fig. 6b, lane 1). On the addition of affinity-purified ICE, p45 was cleaved to yield multiple products (Fig. 6b, lane 2), all of which are congruent with the purified forms of ICE (p24, p20, p10; Fig. 5a) or intermediates predicted to result from single cleavages of the proenzyme. At an inhibitor concentration of 200 nM, cleavage of p45 by affinity-purified ICE was blocked by inhibitor B ( $K_i$ =0.7 nM), but not inhibitor C ( $K_i$ =1  $\mu$ M; Fig. 6b, lanes 3 and 4), indicating that processing was not due to a contaminating protease.

### Effect of peptide aldehyde on mIL-1 $\beta$ release

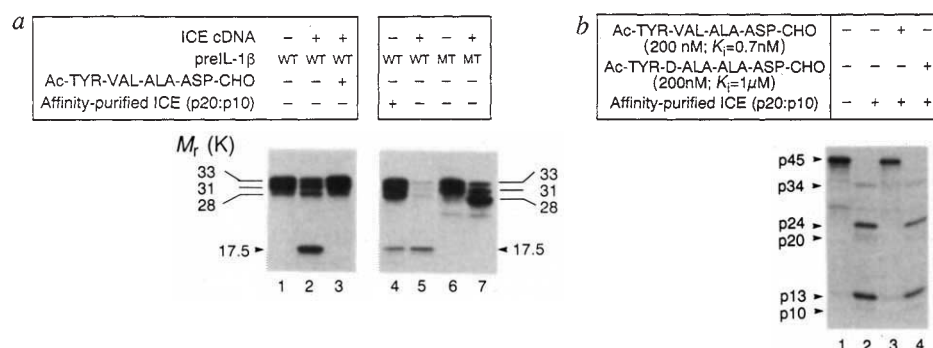
The potency and selectivity of the tetrapeptide aldehyde, inhibitor B, make it a useful inhibitor with which to test the processing function of ICE in intact blood monocytes. Pulse-chase experiments (Fig. 7a) demonstrated that human blood monocytes rapidly synthesize pIL-1 $\beta$  when stimulated with heat-killed *Staphylococcus aureus*<sup>27</sup>. Intracellular pIL-1 $\beta$  chases directly into plasma as mIL-1 $\beta$  with a half-life of 1.5–2.0 h at 30–95% efficiency, depending on the blood donor.

Titration of inhibitor B into human blood caused a dose-dependent decrease in the plasma level of mIL-1 $\beta$  with a 50% inhibitory concentration (IC<sub>50</sub>) of ~4  $\mu$ M (Fig. 7b, d). Although the IC<sub>50</sub> is 5,000  $\times$   $K_i$ , this is consistent with a cytosolic location for ICE and our finding that the peptide aldehyde penetrates cells poorly (unpublished observation). Inhibition was accompanied by a parallel increase in plasma pIL-1 $\beta$ , such that the total amount of secreted IL-1 $\beta$  (mIL-1 $\beta$ +pIL-1 $\beta$ ) remained constant within experimental error (Fig. 7d). The inhibitor had no effect on the intracellular amounts of immunoprecipitable pIL-1 $\beta$  (not shown).

Several controls indicate the specificity of the inhibition. First, the control aldehyde, inhibitor C ( $K_i$ =1.5  $\mu$ M), was considerably less potent (IC<sub>50</sub>>100  $\mu$ M; Fig. 7c, e). Second, other protease inhibitors capable of penetrating cell membranes, including pepstatin, E-64 ((N-(L-3-triscarboxyoxiran-2-carbonyl)-L-leucyl)-amido(4-guanido)butane), a neutrophil elastase inhibitor<sup>12</sup>, and phosphoramidon were without effect at concentrations up to 100  $\mu$ M. Finally, concentrations of inhibitor B up to 100  $\mu$ M had no effect on the plasma levels of IL-6, IL-8 and tumour necrosis factor (TNF- $\alpha$ ), the latter two of which are proteolytically processed<sup>28,29</sup>. These results indicate that ICE alone is responsible for activation of pIL-1 $\beta$ .

FIG. 6 Functional expression and processing of ICE. **a**, ICE activity in lysates from transiently transfected COS-7 cells. Cells transfected with the ICE cDNA (lanes 2, 3, 5, 7) or control vector (lanes 1, 4, 6) were incubated with wild-type (WT) pIL-1 $\beta$  (lanes 1–5) or the mutant (MT) Ala 116 pIL-1 $\beta$  (lanes 6 and 7) synthesized by *in vitro* translation<sup>12</sup>. ICE-transfected cell lysates were also incubated with the inhibitor B, before substrate addition (lane 3). As a control, affinity-purified ICE (2 units) was added to a lysate from cells transfected with the vector alone (lane 4). The sizes of the pIL-1 $\beta$  (33 or 31K) and the ICE-generated cleavage products (28 and 17.5K) are shown. **b**, p45 is cleaved by affinity-purified ICE. Radiolabelled p45 was synthesized in a rabbit reticulocyte lysate (lane 1) and incubated with 10 units of enzyme (lanes 2–4) either alone (lane 2) or with 200 nM inhibitor B or inhibitor C (lanes 3 and 4). Cleavage was assessed by SDS-PAGE.

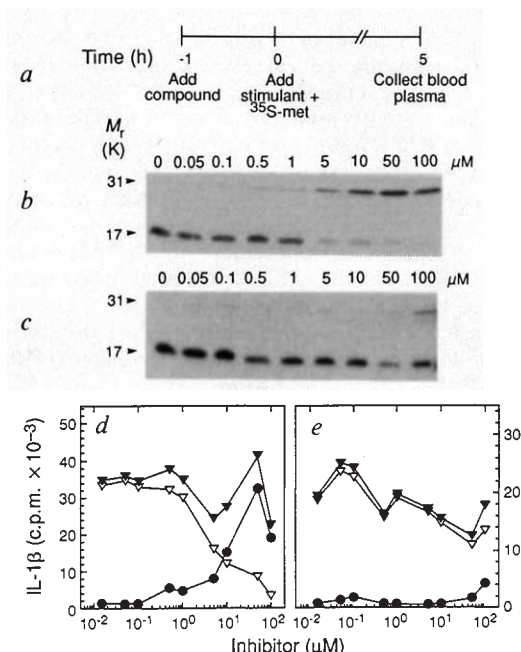
**METHODS.** **a**, The 1.5-kb *Eco*R1 fragment containing the full-length ICE cDNA was cloned into an expression vector under the control of the HIV 5' LTR.



ICE expression plasmid (6  $\mu$ g) and 0.6  $\mu$ g of pXSTAT were cotransfected into COS-7 cells ( $2 \times 10^5$  cells, 40  $\mu$ g Lipofectin) according to the manufacturer's instructions (BRL/GIBCO). Cells were collected 48 h after transfection, lysed in Triton X-100, and assayed for ICE activity<sup>12,24</sup>. **b**, p45-cleavage assays were as follows: 5  $\mu$ l reticulocyte lysate programmed with T7-transcribed ICE RNA was mixed with 10 units affinity-purified ICE alone or with 200 nM of either inhibitor (18 h, 25  $^{\circ}$ C) and analysed as described<sup>12</sup>.

FIG. 7 Inhibition of mature 17.5K IL-1 $\beta$  production by whole human blood monocytes by the tetrapeptide aldehydes, inhibitor B and inhibitor C. *a*, Experimental protocol for pulse-chase experiments. *b*, *c*, SDS-PAGE of immunoprecipitated pIL-1 $\beta$  (31K) and mL-1 $\beta$  (17.5K) after stimulation of whole blood with heat-killed *S. aureus* (HKSA) in the presence of the indicated concentrations of inhibitor B (*b*) or inhibitor C (*c*). *d*, *e*, Plot of c.p.m. in pIL-1 $\beta$  (●) and mL-1 $\beta$  (▽) and the total (▼) of both from *b* and *c*, respectively.

**METHODS.** *a*, Heparinized (10 units ml<sup>-1</sup>) human blood (1 ml) was incubated with the indicated concentration ( $\mu$ M) of one of two tetrapeptide aldehydes (*b*, *d*, inhibitor B  $K_i$  = 0.76 nM; *c*, *e*, inhibitor C,  $K_i$  = 1.5  $\mu$ M), allowed to incubate for 1 h, and then supplemented with 50  $\mu$ Ci [<sup>35</sup>S]methionine (1,076 Ci mmol<sup>-1</sup>) and 10<sup>6</sup> colony-forming units per ml. HKSA. *b*, *c*, After incubation at 37 °C, 5 h, the plasma was removed, immunoprecipitated with mono-specific rabbit anti-hIL-1 $\beta$  IgG, and analysed by SDS-PAGE and fluorography. *d*, *e*, The 31 and 17.5K bands were counted using a radioanalytical imaging system (Ambis Systems) and plotted versus inhibitor concentration. The c.p.m. in the 17.5K bands were multiplied by 1.86 before plotting to correct for the loss of methionine residues on conversion of pIL-1 $\beta$  to mL-1 $\beta$ . Total c.p.m. = c.p.m. pIL-1 $\beta$  + corrected c.p.m. mL-1 $\beta$ .



## Discussion

We have defined here the primary structure, molecular organization and catalytic mechanism of ICE, and established its role in the processing of pIL-1 $\beta$ . The enzyme meets all chemical and catalytic criteria for a cysteine protease, but its sequence is not homologous to any known cellular cysteine protease. It is a heterodimer composed of two subunits, p20 and p10. Although p20 contains the catalytic cysteine, kinetic data provide compelling evidence that both subunits are required for catalytic activity.

The subunits, which are proteolytically derived from a single proenzyme, p45, are flanked by Asp-X bonds. This and the observation that p45 is itself an ICE substrate suggest that activation of ICE is, in part, autocatalytic. That p45 was stable after translation *in vitro* rules out an intramolecular autoprocessing mechanism and suggests that p45 is inactive. Activation of ICE presumably requires limited proteolysis by an unidentified protease, in a manner similar to prostromelysin, before autocatalysis can proceed<sup>30</sup>. The detection of ICE activity in transfected COS-7 cell lysates indicates that p45 can also be activated in non-lymphoid cells.

Consistent with the catalytic mechanism and specificity of ICE, the peptide aldehyde transition state analogue, inhibitor B, is a potent, selective inhibitor ( $K_i$  = 0.76 nM). The selectivity for ICE was demonstrated by affinity chromatography, which enabled >100,000-fold purification of catalytically active enzyme to homogeneity from THP.1 cells. This inhibitor was used to demonstrate that ICE alone is necessary and sufficient for production of mL-1 $\beta$  in human blood monocytes stimulated by heat-killed *S. aureus*. A commensurate increase in the plasma level of pIL-1 $\beta$  accompanied inhibition, indicating that secretion of IL-1 $\beta$  is not mechanistically coupled to the processing function of ICE. Furthermore, the released pIL-1 $\beta$  was stable in blood and did not seem to be susceptible to partial activation by proteases, such as cathepsin G, which are capable of cleaving pIL-1 $\beta$  near Asp 116-Ala 117. Nevertheless, it is possible that such 'bystander' proteases exist at sites of inflammation removed from blood<sup>31</sup>. This uncertainty, and the known ability of IL-1 $\alpha$  and tumour necrosis factor- $\alpha$  to mediate many of the same biological responses as IL-1 $\beta$ , will require studies *in vivo* to assess fully the therapeutic potential of ICE inhibitors. □

Received 6 December 1991; accepted 16 March 1992.

- Hannum, C. H. *et al.* *Nature* **343**, 336–340 (1990).
- Eisenberg, S. P. *et al.* *Nature* **343**, 341–346 (1990).
- Ohlsson, K., Björk, P., Bergenfeldt, M., Hageman, R. & Thompson, R. C. *Nature* **348**, 550–552 (1990).
- Wakabayashi, G. *FASEB J.* **5**, 338–343 (1991).
- Fanslow, W. *Science* **248**, 739–742 (1990).
- McIntyre, K. W. *et al.* *J. exp. Med.* **173**, 931–939 (1991).
- Lonnemann, G. *et al.* *Eur. J. Immun.* **19**, 1531–1536 (1989).
- Mosley, B. S., Dower, S., Gillis, S. & Cosman, D. *Proc. natn. Acad. Sci. U.S.A.* **84**, 4572–4576 (1987).
- Cameron, P., Limjuco, G., Rodkey, J., Bennett, C. & Schmidt, J. A. *J. exp. Med.* **162**, 790–801 (1985).
- Mosley, B. S. *et al.* *J. Biol. Chem.* **262**, 2941–2944 (1987).
- Schmidt, J. A. & Tocci, M. J. in *Peptide Growth Factors and their Receptors I* (eds Sporn, M. B. & Roberts, A. B.) 473–521 (Springer, Berlin, 1990).
- Kostura, M. J. *et al.* *Proc. natn. Acad. Sci. U.S.A.* **86**, 5227–5231 (1989).
- Black, R. A., Kronheim, S. R. & Sleath, P. R. *FEBS Lett.* **247**, 386–390 (1989).
- Howard, A. *et al.* *J. Immun.* **147**, 2964–2969 (1991).
- Griffin, P. R., Coffman, J. A., Hood, L. E. & Yates, J. R. III *Int. J. Mass Spectrom. Ion Phys.* **111**, 131–149 (1991).
- Sleath, P. R., Hendrickson, R. C., Kronheim, S. R., March, C. J. & Black, R. A. *J. Biol. Chem.* **265**, 14526–14528 (1990).
- Kobashi, K. & Horecker, B. L. *Archs Biochem. Biophys.* **121**, 178–186 (1967).
- Rich, D. H. in *Protease Inhibitors* (eds Barrett, A. J. & Salvesen, G.) 153–178 (Elsevier, Amsterdam, 1986).
- Shaw, E. *Adv. Enzym.* **63**, 271–347 (1990).
- Wolfenden, R. *Nature* **223**, 704–705 (1969).
- Morrison, J. F. *Trends biochem. Sci.* **7**, 102–105 (1982).

- Lee, C. C. & Caskey, C. T. *PCR Protocols: A Guide to Methods and Applications* (eds Innis, M. A., Gelfand, D. H., Sninsky, J. J. & White, T. J.) 46–53 (Academic, New York, 1990).
- Kozak, M. *J. Cell Biol.* **108**, 229–241 (1989).
- Hunt, D. F., Yates, J. R. III, Shabanowitz, J., Winston, S. & Hauer, C. R. *Proc. natn. Acad. Sci. U.S.A.* **84**, 620–623 (1987).
- Brenner, S. K. *Nature* **338**, 528–529 (1988).
- Bazan, J. F. & Fletterick, R. J. *FEBS Lett.* **249**, 5–7 (1989).
- Schindler, R., Clark, B. D. & Dinarello, C. A. *J. Biol. Chem.* **265**, 10232–10237 (1990).
- Perez, C. *et al.* *Cell* **63**, 251–258 (1990).
- Clark-Lewis, I., Schumacher, C., Baggiolini, M. & Moser, B. *J. Biol. Chem.* **266**, 23128–23134 (1991).
- Nagase, H., Englund, J. J., Suzuki, K. & Salvesen, G. *Biochemistry* **29**, 5783–5789 (1990).
- Hazuda, D. J., Strickler, J., Kueppers, F., Simon, P. L. & Young, P. R. *J. Biol. Chem.* **265**, 6318–6323 (1990).
- Bull, H. G., Thornberry, N. A. & Cordes, E. H. *J. Biol. Chem.* **260**, 2963–2972 (1985).
- Hewick, R. M., Hunkapiller, M. W., Hood, L. E. & Dreyer, W. J. *J. Biol. Chem.* **256**, 7990–7997 (1981).
- Itoh, N., Tanaka, N., Mihashi, S. & Yamashina, I. *J. Biol. Chem.* **262**, 3132–3135 (1987).
- Sambrook, J., Fritsch, E. F. & Maniatis, T. *Molecular Cloning: A Laboratory Manual* (Cold Spring Harbor Laboratory Press, New York, 1989).
- Bilofsky, H. S. *et al.* *Nucleic Acids Res.* **14**, 1–4 (1986).
- George, D. G., Barker, W. C. & Hunt, L. T. *Nucleic Acids Res.* **14**, 11–15 (1986).
- Devereux, J., Haeblerli, P. & Smithies, O. *Nucleic Acids Res.* **12**, 387–395 (1984).
- Sheridan, R. P. & Venkataraghavan, R. *Proteins* (in the press).
- Gribskov, M., Homyak, M., Edenfield, J. & Eisenberg, D. *Comput. appl. Biosci.* **4**, 61–65 (1988).

**ACKNOWLEDGEMENTS.** We thank K. Swiderek for technical assistance, the staff of Merck Visual Communications for preparation of figures, and B. Buckland, P. Davies, J. Demartino, G. Mark III and A. Williamson for their advice and support.